Since January 2020 Elsevier has created a COVID-19 resource centre with free information in English and Mandarin on the novel coronavirus COVID-19. The COVID-19 resource centre is hosted on Elsevier Connect, the company's public news and information website.

doi:10.1016/j.jmb.2008.11.029 J. Mol. Biol. (2009) 386, 891–901

JMB

Available online at www.sciencedirect.com

ScienceDirect

ELSEVIER

Infectious Bursal Disease Virus: Ribonucleoprotein Complexes of a Double-Stranded RNA Virus

Daniel Luque[1], Irene Saugar[1], María Teresa Rejas[2], José L. Carrascosa[1], José F. Rodríguez[3] and José R. Castón[1]*

[1]*Department of Structure of Macromolecules, Centro Nacional de Biotecnología/CSIC, C/Darwin No. 3, Cantoblanco, E-28049 Madrid, Spain*

[2]*Centro de Biología Molecular (CSIC-UAM), Cantoblanco, 28049 Madrid, Spain*

[3]*Department of Molecular and Cellular Biology, Centro Nacional de Biotecnología/CSIC, Cantoblanco, 28049 Madrid, Spain*

Received 6 October 2008; received in revised form 17 November 2008; accepted 18 November 2008
Available online
25 November 2008

Edited by D. E. Draper

Genome-binding proteins with scaffolding and/or regulatory functions are common in living organisms and include histones in eukaryotic cells, histone-like proteins in some double-stranded DNA (dsDNA) viruses, and the nucleocapsid proteins of single-stranded RNA viruses. dsRNA viruses nevertheless lack these ribonucleoprotein (RNP) complexes and are characterized by sharing an icosahedral $T=2$ core involved in the metabolism and insulation of the dsRNA genome. The birnaviruses, with a bipartite dsRNA genome, constitute a well-established exception and have a single-shelled $T=13$ capsid only. Moreover, as in many negative single-stranded RNA viruses, the genomic dsRNA is bound to a nucleocapsid protein (VP3) and the RNA-dependent RNA polymerase (VPg). We used electron microscopy and functional analysis to characterize these RNP complexes of infectious bursal disease virus, the best characterized member of the Birnaviridae family. Mild disruption of viral particles revealed that VP3, the most abundant core protein, present at ~450 copies per virion, is found in filamentous material tightly associated with the dsRNA. We developed a method to purify RNP and VPg–dsRNA complexes. Analysis of these complexes showed that they are linear molecules containing a constant amount of protein. Sensitivity assays to nucleases indicated that VP3 renders the genomic dsRNA less accessible for RNase III without introducing genome compaction. Additionally, we found that these RNP complexes are functionally competent for RNA synthesis in a capsid-independent manner, in contrast to most dsRNA viruses.

Keywords: IBDV; ribonucleoprotein complex; double-stranded RNA; RNA polymerase activity; innate cellular response

Introduction

Virus evolution has resulted in an extraordinary diversity of replication strategies and life cycles.[1] Whereas the genetic information for eukaryotic and prokaryotic cells is contained in double-stranded DNA (dsDNA), viral genomes are less constrained and exhibit greater diversity. The different virus families have genomes formed by dsDNA or single-stranded DNA (ssDNA), dsRNA or ssRNA, with (1) positive, negative, or ambisense polarity, (2) circular or linear topology, and (3) single or multipartite genomes. ssRNA and dsRNA viruses must provide an appropriate RNA-dependent RNA polymerase (RdRp) to replicate their genomes, and RNA duplex replication intermediates are usually synthesized during viral infection. dsRNA is nonetheless a potent signal for the induction of intracellular defense mechanisms in higher eukaryotes,[2,3] and viruses have adopted different dsRNA sequestration mechanisms. dsRNA viruses never release their genome from a specialized capsid with an unusual $T=2$ symmetry, where both the positive and negative strands are synthesized but freshly

*Corresponding author. E-mail address: jrcaston@cnb.csic.es.

Present address: D. Luque, Kapsid Link SL, Alcalá 420, 28017 Madrid, Spain; I. Saugar, Cancer Research UK, Clare Hall Laboratories, South Mimms, Herts EN6 3LD, UK.

Abbreviations used: BSA, bovine serum albumin; dsDNA/RNA, double-stranded DNA/RNA; IBDV, infectious bursal disease virus; IPNV, infectious pancreatic necrosis virus; ORF, open-reading frame; PBS, phosphate-buffered saline; RdRp, RNA-dependent RNA polymerase; RNP, ribonucleoprotein; ssDNA/RNA, single-stranded DNA/RNA.

synthesized transcripts are extruded into the cell cytoplasm to be translated.[4] Positive-strand RNA viruses limit the negative-strand synthesis to very low levels, and replicative intermediates containing dsRNA regions are scarcely accumulated. Furthermore, many plant and insect positive-sense RNA viruses express a dsRNA-binding protein that acts as a potent suppressor, inhibiting host RNA silencing.[5,6] In contrast, negative-strand viruses, which need massive amounts of both positive-stranded RNA and negative-stranded RNA to be used as messages and progeny genomes, usually prevent formation of an RNA duplex by shielding the genomic (−) ssRNA with the viral nucleocapsid (N) protein, forming a ribonucleoprotein (RNP) complex.[7,8]

Infectious bursal disease virus (IBDV), an avian pathogen, belongs to the Birnaviridae family of nonenveloped icosahedral viruses,[9] which have a bipartite dsRNA genome (segments A and B of 3.2 and 2.8 kbp, respectively) enclosed within a single-layered capsid with $T=13l$ geometry.[10–12] Results from our laboratory indicate that IBDV is an icosahedral dsRNA virus that can package more than one complete genome copy (Luque, D., Rivas, G., Alfonso, C., Carrascosa, J. L., Rodríguez, J. F. & Castón, J. R. (2009). Infectious Bursal Disease Virus: an icosahedral polyploidy dsRNA virus. *Proc. Natl. Acad. Sci. USA*. In press). Our analyses focused on E5 IBDV virions, the most abundant population in an infected cell, which package four dsRNA segments.

IBDV segment A has two open-reading frames (ORFs). The short ORF encodes VP5, a nonstructural polypeptide involved in virus egress. The long ORF codes for a polyprotein that is processed by its viral protease, VP4, a common feature of positive-sense ssRNA viruses. This yields most of the structural proteins, including the capsid precursor protein pVP2, VP3, and VP4.[13,14] pVP2 is further processed at the C-terminal region during virus maturation into VP2, which assembles into trimers, the structural unit of the virion capsid. Segment B (2.8 kbp) encodes VP1, the RdRp,[15,16] which is present in the virion as a free protein or covalently linked to the 5′ ends of the two genome segments (the so-called VPg).

Much of our understanding of birnaviruses, which lack the $T=2$ core usually found in dsRNA viruses, is based on studies of IBDV and infectious pancreatic necrosis virus (IPNV), a pathogen of aquatic fauna that shares many molecular properties with IBDV. VP3 (256 residues) is a multitasking protein that has several activities throughout the viral life cycle. In addition to being a self-interacting protein,[17] VP3, mediated by its last five mainly acidic residues, interacts with pVP2 during particle morphogenesis.[18,19] In addition, mediated by the 16 C-terminal-most residues, VP3 interacts with VP1[20–22] independently of the presence of dsRNA. VP3 is also an RNA-binding protein,[23,24] and its atomic structure was recently solved by X-ray crystallography to 2.3 Å.[25] The VP3 central region (residues 92–220) is organized as a dimer in the

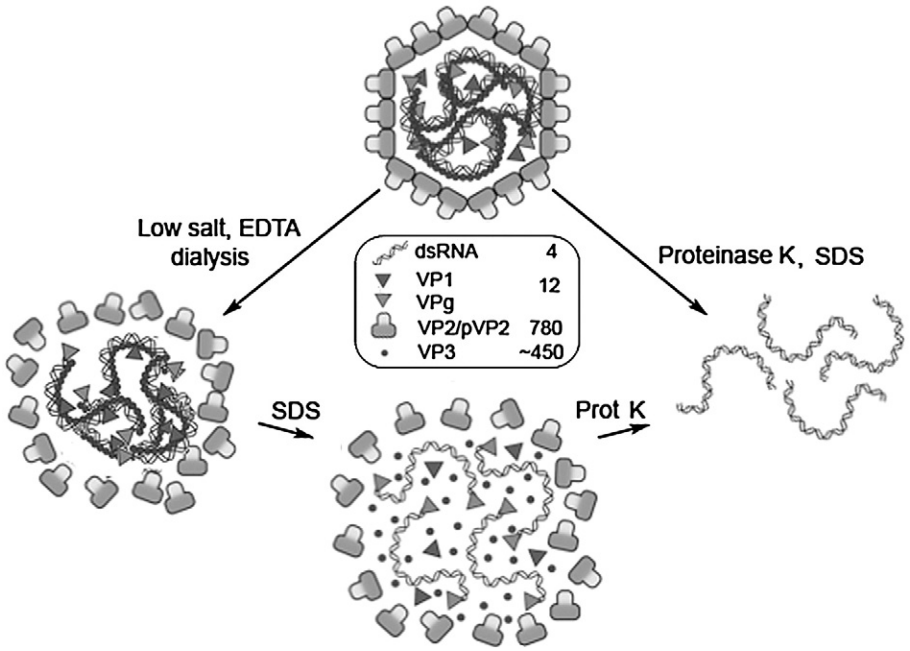

Fig. 1. IBDV model and virion destabilizing treatments to obtain RNP, VPg–dsRNA complexes, and dsRNA. The scheme represents the IBDV model with its associated stoichiometry for the major structural components. This scheme is adapted from the work of Ahlquist.[28] A polyploid virion with four packaged dsRNA segments is shown as E5 IBDV particles. Dialysis of IBDV virions against low-salt buffer in the presence of EDTA renders structurally preserved RNP (constituted by dsRNA, VP3, and VP1/VPg) and soluble capsid protein subunits of VP2/pVP2 (left arrow); treatment of these RNP crude preparations with SDS releases VP3 and noncovalently bound VP1 subunits as soluble components and VPg–dsRNA complexes. Treatment of these crude VPg–dsRNA preparations with proteinase K would eventually render dsRNA molecules. Incubation of E5 IBDV virions with SDS and proteinase K releases dsRNA segments (right arrow).

crystal and is folded into two α-helical domains connected by a long hinge. One of these domains shows similarity to transcription regulation factors.

Previous descriptions of IPNV reported RNP filaments containing VP3 and the viral dsRNA after low-salt treatment of virions.[26] This feature is unique among dsRNA viruses and might suggest a functional link with negative-sense ssRNA viruses, in which RNPs are commonly found. Birnavirus capsid and RdRp proteins are unexpectedly similar to their corresponding counterparts in some positive-sense ssRNA viruses, such as nodaviruses and tetraviruses.[11,27]

Here, we used several approaches for structural and functional characterization of VP3 interactions with dsRNA and VP1 in IBDV. We developed a purification method rendering stable RNP, whose reproducibility is easily monitored by retarding electrophoretic analysis. The dsRNA-binding properties of VP3 make the genomic dsRNA less accessible to RNase III without introducing genome compaction. In addition, the purified RNP of IBDV is functional in transcription and/or replication, and its integrity is required for RdRp activity.

Results

Morphology and electrophoretic characterization of disrupted IBDV virions

Treatment of purified IPNV viral particles in very-low-salt conditions disrupts the particle, with loss of a filamentous material that corresponds to RNP.[26] Figure 1 shows a scheme of the alternative treatments to which purified IBDV virions were subjected to render dsRNA molecules with different associated viral proteins. In a similar procedure, dialysis of purified IBDV E5 full virions against a low-salt buffer in the presence of EDTA (ethylenediaminetetraacetic acid) ruptured most particles to release RNPs. These RNPs consisted of dsRNA molecules complexed with several proteins (below). If this material was incubated with SDS, noncovalent interactions were altered such that VP3 protein was released and VPg–dsRNA complexes were obtained. Finally, purified dsRNA segments were obtained from E5 particles treated with SDS and proteinase K. Crude preparations of IBDV RNP were analyzed by electron microscopy and negative staining (Fig. 2a) or by metal shadowing (Fig. 2b). In these conditions, a granular material that probably corresponds to disassembled capsid units surrounded the ~9-nm-thick RNP filaments, as estimated from metal-shadowed filaments.

We used agarose gel electrophoresis and ethidium bromide staining to study dsRNA interactions with viral proteins from freshly disrupted particles. For that, dsRNA band mobility shifts were analyzed under native conditions in the absence of SDS (Fig. 3a, left) and under denaturing conditions in the presence of 0.1% SDS (Fig. 3a, right). A scheme showing the macromolecular complexes analyzed is given in Fig. 3b. The existence of a single band of defined mobility demonstrated the structural integrity of the virion particles (Fig. 3a, lane 1). Purified dsRNA segments A and B were observed as two well-defined bands (Fig. 3a, lane 2). dsRNA from SDS-treated virions, in which all interactions are broken except for covalent links, was visualized as two retarded bands under denaturing conditions, indicating the presence of VP1–dsRNA complexes (VPg–dsRNA; Fig. 3a, lane 3, right). VPg–dsRNA complexes nonetheless appeared as an unresolved band with a large smear if SDS is absent in the agarose gel (Fig. 3a, lane 3, left). Filamentous particles identified as the putative IBDV RNP (i.e., VPg–dsRNA complexes shielded by VP3 molecules)

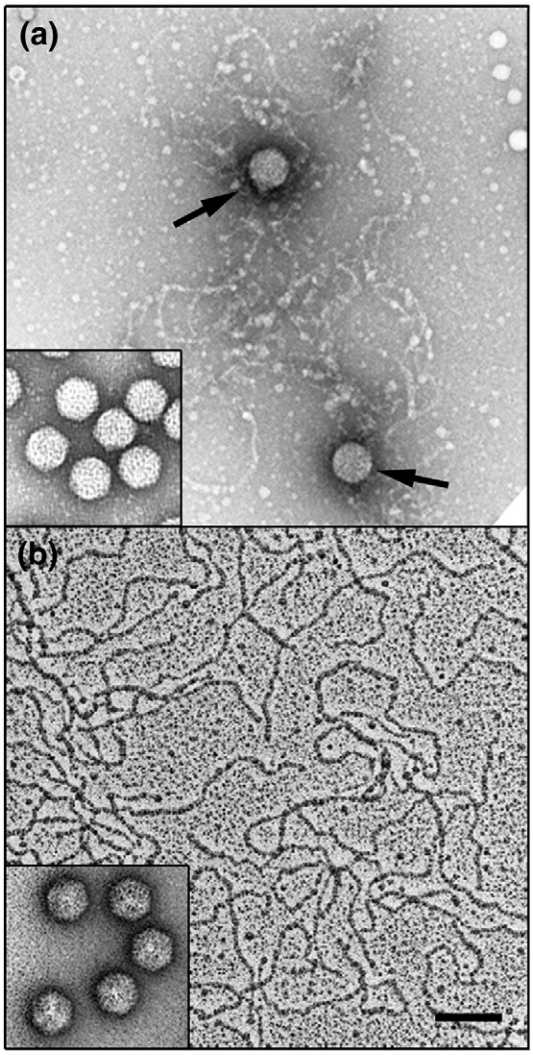

Fig. 2. Electron microscopy of disrupted IBDV particles by low-salt treatment. E5 IBDV virions were dialyzed against low-salt buffer and directly processed for electron microscopy by (a) negative staining with 2% uranyl acetate or (b) air drying and metal shadowing. Arrows indicate unaltered virions. Insets show general views of virions dialyzed against PES buffer and therefore structurally well-preserved particles. Bar represents 100 nm.

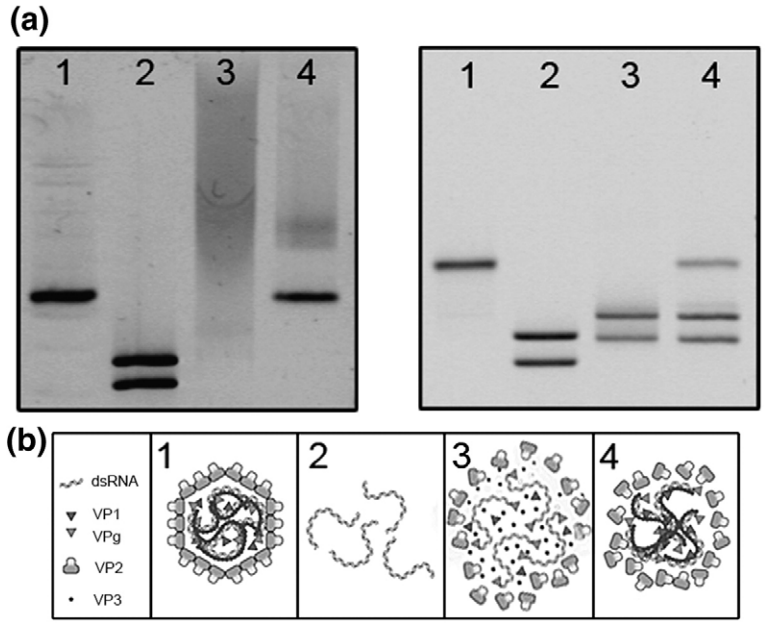

Fig. 3. Electrophoretic characterization of IBDV-derived RNP complexes. (a) Agarose gel electrophoresis in the absence (left) or in the presence (right) of 0.1% SDS of IBDV-derived complexes: 1, structurally unaltered virions; 2, dsRNA genome molecules; 3, unpurified VPg–dsRNA complexes; and 4, disassembled virions with structurally preserved RNP. (b) Cartoon illustrating the different assemblies analyzed in this study (1–4, as described above). This scheme was adapted from the work of Ahlquist.[28]

gave rise to two bands with a more reduced mobility, as well as another band that migrated similarly to intact virions in native conditions (Fig. 3a, lane 4, left). Finally, in denaturing conditions, RNP behaved like VPg–dsRNA complexes (the two faster migrating bands) and intact virions (the slower migrating band) (Fig. 3a, lane 4, right). Western blot of these agarose gels containing the purified virions, dsRNA molecules, as well as crude preparations of VPg–dsRNA and RNP complexes, using anti-VP1 (αVP1), anti-VP2 (αVP2), and anti-VP3 (αVP3) antisera, confirmed their biochemical composition (Supplemental Data).

Purification of IBDV RNP and VPg–dsRNA complexes

RNP and VPg–dsRNA complexes were purified from disrupted virions by ultracentrifugation, alone or with detergent (0.1% SDS), in glycerol step gradients (Fig. 4). Fractions were collected from top to bottom and characterized by native agarose gel electrophoresis and ethidium bromide staining (Fig. 4a and c) and by SDS-PAGE and Western blot using specific αVP1, αVP2, and αVP3 antibodies (Fig. 4b). In these conditions, RNPs were recovered mainly in the middle fractions (fractions 5–7) showing two well-

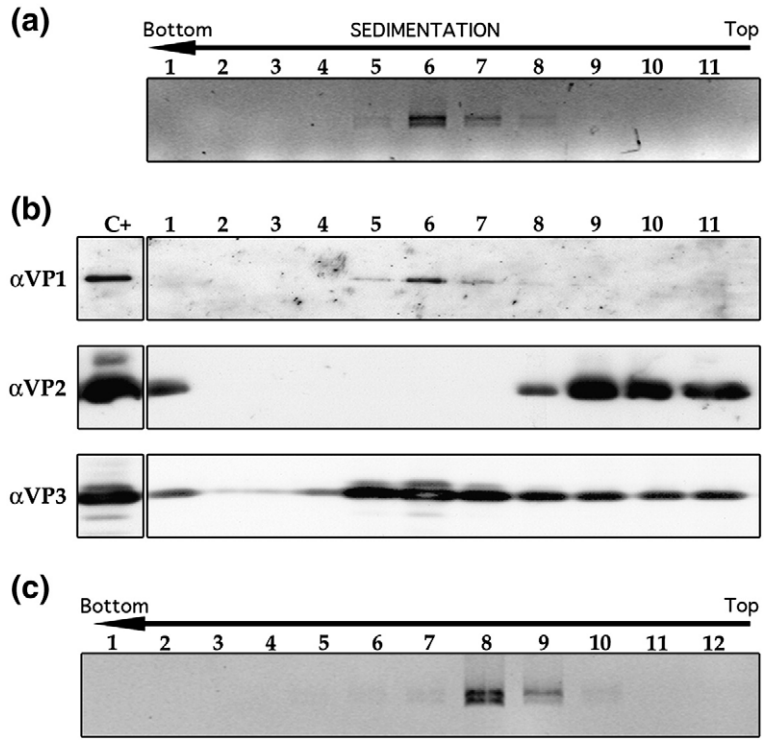

Fig. 4. Purification of RNP and VPg–dsRNA complexes. (a and b) RNPs from dissociated virions by low-salt dialysis were purified by glycerol gradient centrifugation; 11 fractions were collected, analyzed by SDS-PAGE, and developed by (a) Coomassie staining or (b) Western blotting with αVP1 (top, αVP1), αVP2 (middle, αVP2), or αVP3 (bottom, αVP3) antibodies. (c) Typical profile of VPg–dsRNA complexes purified from dissociated virions in the presence of SDS. The direction of sedimentation was from right to left, with fraction 11 (or 12) representing the top of each gradient.

defined bands that could correspond to RNP-A and RNP-B of segments A and B, respectively (Fig. 4a). Whereas VP1 and much of VP3 comigrated with the viral dsRNA, VP2 was found either in the bottom fractions (associated with a minor fraction of intact or partially disrupted capsids) or in the top fractions (corresponding with soluble capsid proteins) (Fig. 4b).

VPg–dsRNA complexes, developed by ethidium bromide staining, were purified by a similar procedure in the presence of SDS (Fig. 4c). Equivalent analysis by SDS-PAGE and Western blot confirmed that VP1 is the only protein component of these complexes (not shown).

Characterization and RNase digestion of RNP and VPg–dsRNA complexes

The homogeneity and stability of these IBDV nucleic acid preparations (dsRNA, VPg–dsRNA, and RNP) must be monitored to study their functional and structural aspects. We used the procedures described above to analyze electrophoretic mobility shift under native conditions in agarose gels (Fig. 5a, top). Purified VPg–dsRNA complexes were found as two well-defined bands (Fig. 5a, lane 3) that migrated more slowly than did those of purified segments A and B (Fig. 5a, lane 2). Purified RNP gave rise to the two slowest migrating bands (Fig. 5a, lane 4). Western blot analyses of these agarose gels, using IBDV particles as the internal positive control, verified the identity of the viral proteins in these complexes (αVP1, αVP2, and αVP3; Fig. 5a). The fact that VPg–dsRNA complexes and RNPs were consistently visualized as two well-defined bands indicates that a constant amount of protein is bound to segments A and B.

To determine whether VP3 protects dsRNA molecules in the RNP filaments, we conducted accessibility experiments with RNase III, a nuclease specific for dsRNA. The IBDV genome within virion particles (negative control) was RNase III resistant (Fig. 5b, 1), in contrast to the extensive digestion of the positive control with purified IBDV dsRNA (Fig. 5b, 2) and VPg–dsRNA complexes (Fig. 5b, 3). RNPs were more resistant to degradation, and defined smaller fragments were not detected (Fig. 5b, 4). Higher RNase III concentrations nonetheless led to total digestion of the dsRNA in RNPs. These results imply that dsRNA is homogeneously shielded by VP3, consistent with previous thickness measurements from metal-shadowed filaments.

VP3 does not condense dsRNA

dsRNA, VPg–dsRNA complexes, and RNP, whose structural integrities were confirmed by parallel monitoring of their electrophoretic mobilities, were further characterized by metal shadowing and electron microscopy (Fig. 6a, c, and e). At appropriate dilutions, we were able to measure the lengths and differences in diameter of these filamentous particles. Data obtained for these purified filaments revealed two components with mean lengths of ~0.975 and ~0.85 μm (Fig. 6b, d, and f). These results are compatible with an A-type duplex (pitch = 2.81–3 Å), since segments A (3.2 kbp) and B (2.8 kbp) measured 0.9–0.96 and 0.79–0.84 μm, respectively, indicating that VP3 binding does not condense the viral genome. In addition, whereas purified dsRNA molecules and VPg–dsRNA complexes have a fairly uniform diameter (65.3±1.8 and 64.8±5.7 Å, respectively), RNPs were much thicker (~97.1±3.2 Å), as

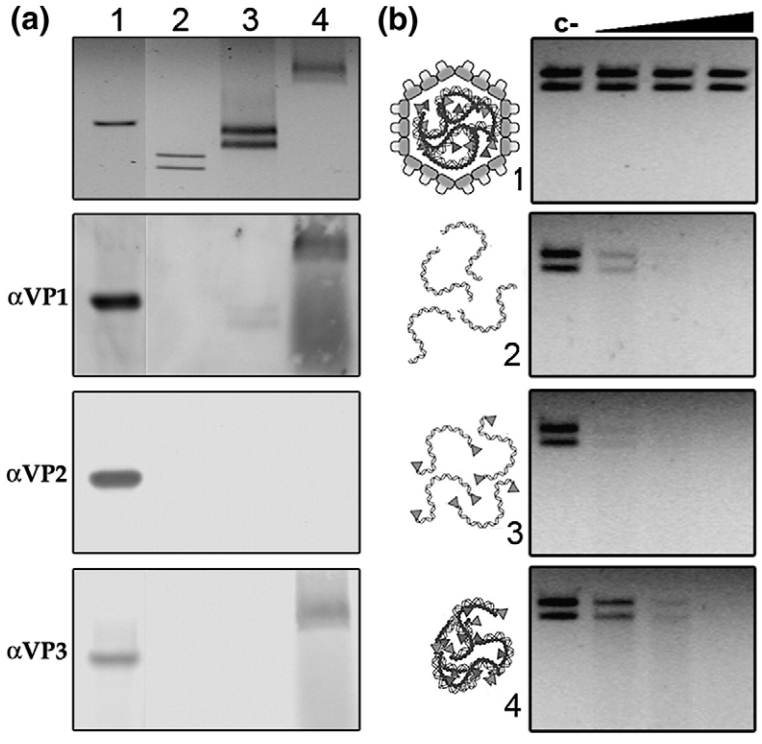

Fig. 5. Biochemical characterization of purified IBDV RNP. (a) Agarose gel electrophoresis of (1) virions, (2) genome dsRNA molecules, (3) VPg–dsRNA complexes, and (4) RNPs visualized by bromide ethidium staining (top) or by Western blotting with αVP1 (top, αVP1), αVP2 (middle, αVP2), or αVP3 (bottom, αVP3) antibodies. (b) RNase III accessibility for IBDV dsRNA: (1) dsRNA in intact full E5 particles, (2) purified dsRNA, (3) dsRNA from VPg–dsRNA complexes, and (4) dsRNA from purified RNP were treated with increasing amounts of RNase III (from left to right). Lane c− shows controls for each experiment without RNase III treatment. Schematic cartoons are the same as those used in Fig. 2.

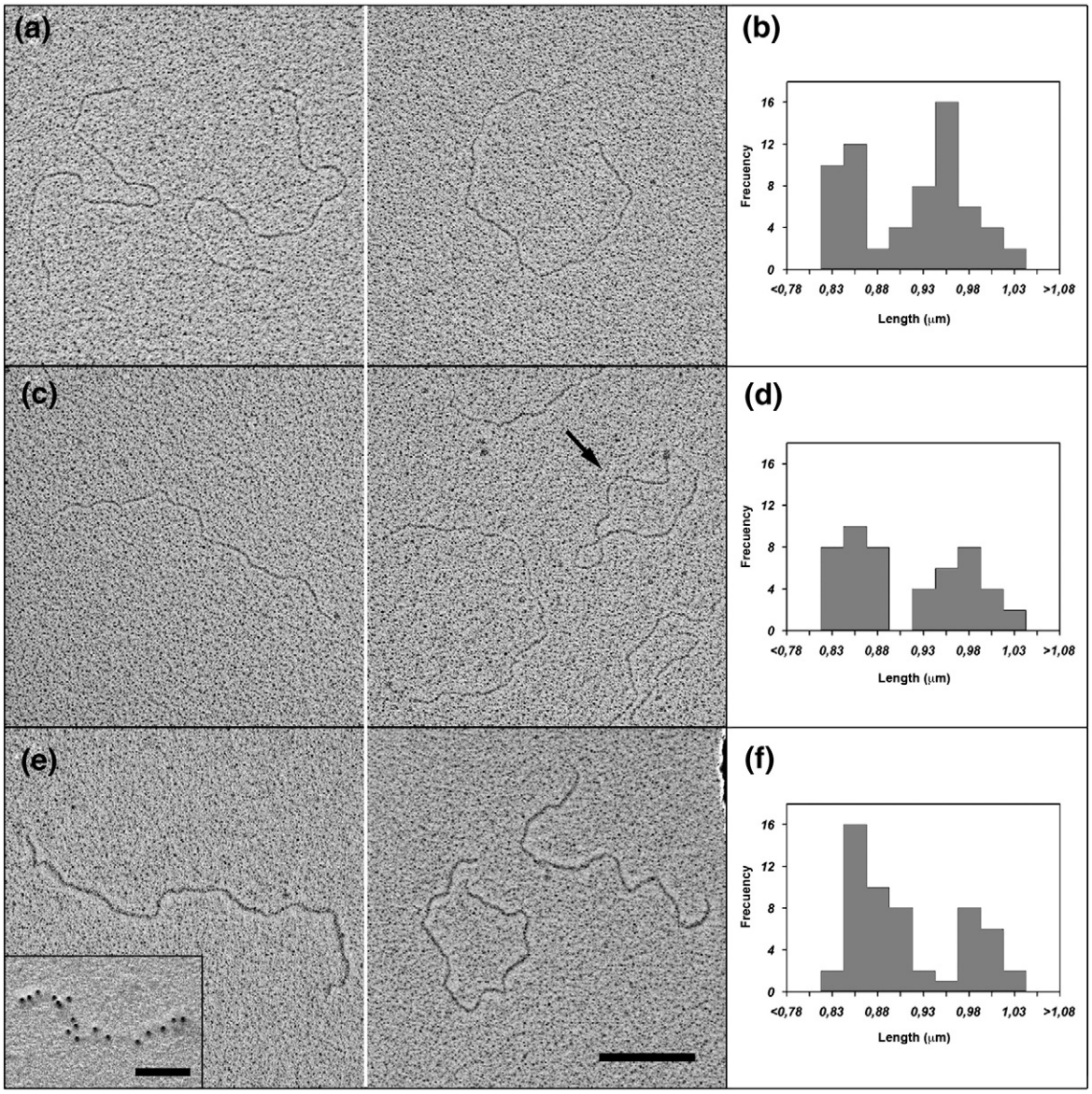

Fig. 6. Lengths of dsRNA molecules, VPg–dsRNA complexes, and RNPs. (a and b) Electron micrographs of metal-shadowed purified dsRNA molecules and the histogram of length measurements made from these micrographs ($n = 62$). (c and d) Electron micrographs of shadowed purified VPg–dsRNA complexes and the corresponding histogram ($n = 50$). The arrow indicates a circularized VPg–dsRNA complex, occasionally visualized. (e and f) Electron micrographs of shadowed purified RNP and the corresponding histogram ($n = 55$). Inset shows immunogold-labeled and shadowed RNPs after incubation with αVP3 antiserum and protein A conjugated to 5-nm colloidal gold particles. Bar represents 200 nm.

determined in crude RNP samples. Immunolabeling of RNP with αVP3 antiserum (Fig. 6e, inset) corroborated this increase in diameter, as gold particles were located homogeneously along the RNP filaments.

Only a fraction (~30%) of the VPg–dsRNA complexes were visualized clearly as circular structures (Fig. 6c, arrow), in contrast with the dsRNA molecules and RNPs, which were always linear. Considering that VPg–dsRNA complexes were purified under denaturing conditions, circularized molecules might be artifactual, due to denatured VPg. The morphology of RNP analyzed under nondenaturing conditions (close to its native state) suggests that native viral dsRNA is linear, not circular, as previously proposed.[29]

RNA polymerase activity of RNP complexes

RdRp activity of the IBDV VP1 was assessed using as template the dsRNA molecules of the complexes characterized in this study (Fig. 7). The products of VP1 catalytic activity for the reactions containing RNPs or virions (positive control) were visualized as two radioactively labeled bands (Fig. 7, inset). Virions and RNPs showed a similar activity profile for [α-^{32}P]UTP incorporation, with the highest activity during the first 30 min. Reactions containing VPg–dsRNA complexes (obtained under denaturing conditions) were similar to those performed with purified dsRNA in the absence of VP1 (negative control). These results show that although a minor

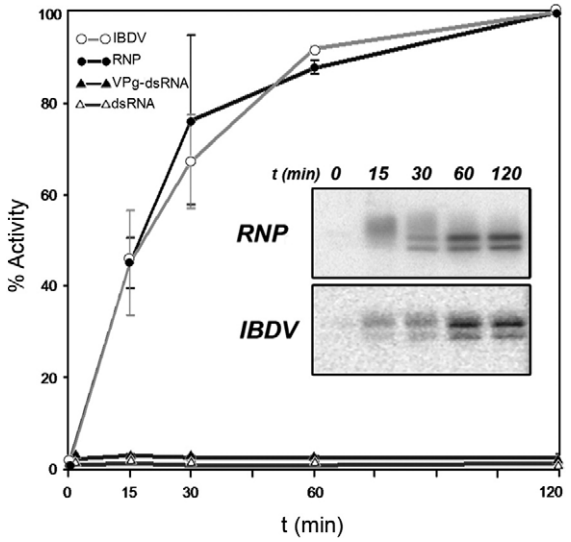

Fig. 7. IBDV RdRp activity. RNA polymerase activity was determined on the [α-^{32}P]UTP incorporated to the reaction products that were separated on 0.7% agarose gel. Mixture reactions were supplemented with full virions (IBDV), RNP complexes, VPg–dsRNA complexes, or purified dsRNA molecules. Each measurement corresponds to the mean value from four independent experiments such that the highest value obtained corresponds to 100%. Insets show autoradiography of the reaction products for a single experiment performed with RNP complexes or full virions (IBDV).

VP3 fraction was lost during RNP purification (Fig. 4b), RNPs are functionally competent for RNA synthesis in the absence of either the VP2 capsid protein or a structurally unaltered capsid.

Discussion

We performed structural and functional characterization of the IBDV RNP genome segments. Several earlier studies demonstrated that VP3 plays a double scaffolding role by interacting with the precursor form of the capsid protein pVP2 for correct capsid assembly[18,19,30,31] and by stabilizing both segments of genomic dsRNA.[22,24] VP3 is found in IBDV virions at a relatively constant copy number (~450 copies), independently of the number of packaged dsRNA segments. Incorporation of VP3 therefore appears to be determined mainly by its role as a scaffolding protein during capsid assembly.[18]

VP3 is a multitasking protein: a moonlighting protein?

The scaffolding VP3-associated activities have been located in its C-terminal region, which also participates in VP1 recruitment into the capsid and promotes conformational change of a VP1 loop that removes the inherent structural blockade of the polymerase active site, thus serving as a transcriptional activator.[20] In addition, the VP3 oligomerization domain maps within the 42 C-terminal residues of the polypeptide,[21] indicating further functional complexity. In addition to this oligomerization domain, VP3 has an independent dimerization domain mediated by a number of residues within the central region of VP3.[25] Structural studies by three-dimensional cryo-electron microscopy are under way to determine whether the RNP filaments are dsRNA molecules wrapped with VP3 monomers, dimers, or higher-order oligomers formed by multimerization of preformed VP3 dimers.

VP3 has a highly hydrophilic C-terminal tail region that is rich in charged amino acids and proline residues. This C-terminal tail was predicted to be well exposed and disordered and consequently able to bind proteins and nucleic acids. VP3 may be considered an example of a moonlighting protein that can carry out multiple, apparently unrelated functions.[32] Moonlighting proteins represent a means of increased complexity for viruses with limited coding capacity. Although the mechanisms of classical moonlighting rely on the use of separate surfaces for binding different partners and/or catalyzing distinct reactions, VP3 uses close or overlapping interaction regions to exert diverse effects. Reports are becoming more frequent of intrinsically unstructured proteins that are able to perform several functions,[33] as predicted here for the VP3 C-terminal region, which is invisible in the reported atomic structure of VP3, similar to the C-terminal domain of a transcriptional corepressor, CtBP.[34] Switching mechanisms among these VP3 functions are poorly understood. Coordination of their activities might be achieved by conformational changes in partner-induced processes (pVP2, VP1, dsRNA, or some combination of these), variations in oligomeric state, transient folded/unfolded states, local concentration of a ligand at the viroplasms, or a combination of these possibilities.

Moonlighting proteins such as VP3 are potentially the best target candidates for rational drug design because a single compound will interfere with several functions throughout the viral life cycle, as confirmed by some previous studies.[35]

Viral nucleic acid-binding proteins

Viral proteins that interact with nucleic acids to mediate selection, packaging, and/or condensation within the viral capsid are relatively common in the different virus families. VP3 interaction with the viral dsRNA-forming RNP complexes is nonetheless a unique feature among dsRNA viruses. The IBDV core RNP morphology is somewhat reminiscent of that of the nucleoproteins of certain dsDNA viruses. Polyomavirus and papovavirus (e.g., SV40) are icosahedral particles that contain within their capsids a mini chromosome in which circular dsDNA is folded into nucleosomes by cellular core histones. Similarly, the adenovirus core contains a copy of linear dsDNA; it has no cellular histone but has virus-specific proteins. Polypeptide VII, the major core protein, is tightly bound to DNA, giving a beaded appearance with a morphology similar to cell chromatin.[36]

VP3 molecules interact along the dsRNA molecule without introducing the longitudinal compression described for cellular heterochromatin. Nevertheless, in this scenario, VP3 might compact the genome at the interior capsid through intermolecular interactions. The ability of VP3 to oligomerize supports this hypothesis; under certain conditions (i.e., in the presence of glycerol or Mg^{2+}), we detected thicker RNP filaments (not shown). Definition of RNP and VPg–dsRNA complexes at two well-defined electrophoretic mobility bands implies that, in addition to the covalently bound VPg, all dsRNA molecules have the same number of VP3 molecules. The most abundant class of IBDV particles is formed by the E5 population that encapsidates four dsRNA segments such that each segment is bound to ~110 VP3 molecules, yielding a ratio of 26 bp/molecule of VP3 (Luque, D., Rivas, G., Alfonso, C., Carrascosa, J. L., Rodríguez, J. F. & Castón, J. R. (2009). Infectious Bursal Disease Virus: an icosahedral polyploidy dsRNA virus. *Proc. Natl. Acad. Sci. USA*. In press). This ratio, calculated assuming that 100% of VP3 molecules are bound to dsRNA, is relatively low as compared with the nucleocapsid protein of the paramyxovirus Sendai virus, which is bound to six ribonucleotides.[37] We are also working on the functional analysis to determine at what ratio the RNP properties become evident. The appearance of the RNP of negative-sense (e.g., filovirus, rhabdovirus, paramyxovirus, and orthomyxovirus) and positive-sense (e.g., coronaviruses) ssRNA viruses is highly variable, depending on salt concentration, deletion of specific C- or N-terminal regions, and/or the presence of specific ions. These RNPs form constrained, tightly packed coils with a fairly uniform diameter or flexible, extended linear structures.[38–40]

T=2 core *versus* RNP complexes

dsRNA viruses share a structurally conserved core with $T=2$ symmetry that surrounds the genome and whose structural integrity remains undisturbed throughout the viral cycle. Negative-strand and positive-strand syntheses occur within the $T=2$ capsid, where the viral RNA polymerase is incorporated as an integral component. To avoid suppression of virus gene expression, the $T=2$ capsid isolates dsRNA molecules or replicative intermediates from host molecules, preventing intracellular responses such as protein kinase R-mediated responses[3] and RNA interference mechanisms. All members of the Birnaviridae family lack the $T=2$ core, and it is plausible that RNPs have acquired some functions associated to the $T=2$ capsid. Our analyses demonstrate that, in contrast to most dsRNA viruses,[41] IBDV RNPs are functionally competent for RNA synthesis in a capsid-independent manner (and in the absence of VP2). The catalytic activity of VP1 is increased fivefold when VP3 is present,[20] resembling results obtained with negative-sense ssRNA viruses, in which the nucleoprotein–RNA complex (and not the naked viral RNA) serves as the actual template for the RdRp.

RNPs show low sensitivity to RNase degradation and behave similarly to the replication and transcription complexes of some positive-sense ssRNA viruses.[28,42] VP3–dsRNA interaction might protect genomic dsRNA from processing by RNA-induced silencing complexes.[2,43] Studies are currently under way to verify whether VP3 is an effective suppressor of viral RNA silencing *in vivo* and whether the virion capsid is disassembled after cell entry.

Compared with other dsRNA viruses, all these IBDV features involve a clearly different genome organization, as well as a previously unreported replication strategy.

Materials and Methods

Virion purification

IBDV strain Soroa was purified from QM7 quail muscle cells and stored in PES buffer [25 mM piperazine-*N*,*N*′-bis (2-ethanesulfonic acid), pH 6.2, 150 mM NaCl, and 20 mM $CaCl_2$]. IBDV particles from the cell medium were precipitated with 3.5% polyethylene glycol 6000 and 0.5 M NaCl, and the resulting pellet was resuspended in PES buffer. Particles were then pelleted through a 25% (wt/wt) sucrose cushion (37,000 rpm, 2.5 h, 4 °C) in a Beckman-Coulter SW41 rotor, followed by CsCl equilibrium gradient centrifugation (40,000 rpm, 14 h, 4 °C) in a Beckman-Coulter NVT65 rotor, adjusting the initial density of the solution to 1.33 g/ml by CsCl addition. Six virus-containing bands were visible (designated as E1 to E6 from top to bottom), and E5 viral particles (the major band) were collected by needle insertion and aspiration into a syringe. E5 aliquots were dialyzed against the PES buffer and stored at 4 °C for a maximum of 2–3 weeks.

Purification of RNP, VPg–dsRNA complexes, and dsRNA from IBDV virions

RNP complexes were purified from disrupted E5 viral particles obtained by dialysis against a low-ionic-strength buffer (5 mM Tris–HCl, pH 8.0, and 5 mM EDTA) for 18 h at room temperature. This extract (~200 μl) was centrifuged in a glycerol step gradient [0.5 ml of 70% (wt/vol) glycerol, 0.75 ml of 50% glycerol, 0.375 ml of 40% glycerol, and 1.2 ml of 33% glycerol] in an SW55 rotor (40,000 rpm, 2 h, 4 °C). The same protocol was used for VPg–dsRNA complex purification, except that all buffers contained 0.1% SDS and samples were ultracentrifuged for 4 h.

E5 particles were incubated with 1% SDS (3 min, 100 °C) and treated with proteinase K (2 mg/ml, 1 h, 37 °C) to analyze dsRNA molecules. dsRNA was then extracted with TriZol (Invitrogen) and purified using silica-based mini-spin columns (Quiagen).

Agarose gel electrophoresis

Purified virions, dsRNA–protein complexes, and nucleic acids were incubated with 6× blue/orange loading dye (Promega; 10 mM Tris–HCl, pH 7.5, 0.4% orange G, 0.03% bromophenol blue, 0.03% xylene cyanol FF, 15% Ficoll 400, and 50 mM EDTA). Samples were loaded onto 0.7% agarose gels in 90 mM Tris–HCl, pH 8.0, 90 mM boric acid, and 20 mM EDTA. When indicated, 0.1% SDS was added to the gel. Electrophoresis was carried out at 4 °C in

the same buffer used to prepare the gel until the dye reached the bottom of the gel. After electrophoresis, samples were visualized with ethidium bromide.

SDS-PAGE

Glycerol gradient fractions were added to a Laemmli sample buffer to 1× final concentration (62.5 mM Tris–HCl, 2% SDS, 5% glycerol, 0.012% bromophenol blue, and 2 mM DTT, pH 6.8), heated (3 min, 100 °C), chilled on ice (1 min), and analyzed in 11% SDS-PAGE.

Western blot

Western blot analyses were carried out at room temperature. Samples separated on agarose or polyacrylamide gels were incubated in 48 mM Tris–HCl, 39 mM glycine, 0.0375% SDS, and 20% methanol and then transferred to a nitrocellulose membrane (Protran, Schleicher & Schuell) in a semidry electroblotter (SD cell, BioRad) for 45 min at 200 mA. Blots were then treated with blocking solution [phosphate-buffered saline (PBS) containing 5% nonfat dry milk] for 30 min and with primary rabbit antibodies (αVP1, αVP2, or αVP3) diluted in blocking solution for 2 h. The membrane was washed three times in blocking solution and incubated with a horseradish peroxidase-conjugated goat anti-rabbit antibody (diluted 1:5000; GE Healthcare) for 2 h. Membranes were washed extensively and developed with ECL chemiluminescence reagent (GE Healthcare) or with a peroxidase substrate [0.05% 4-cloro-1-naphtol, 0.025% H_2O_2 (30%), and 16% DMSO in PBS].

RNase III sensitivity assay

RNase III is specific exclusively for dsRNA. RNase protection assays were performed with equivalent amounts of three samples (dsRNA, VPg–dsRNA, and RNP) purified from freshly prepared IBDV virions. The reaction buffer [50 mM Tris–HCl, pH 8.0, 150 mM NaCl, 20 mM $MnCl_2$, and 0.3 mg bovine serum albumin (BSA)/ml] containing 0, 125, 500, or 2000 mU of ShortCut RNase III (New England Biolabs) and ~0.1 μg of dsRNA was incubated (30 min, 37 °C). Reactions were terminated by addition of 50 mM EDTA and 0.1% SDS, boiled for 3 min, and cooled at 4 °C for 1 min. Samples were incubated with 0.2 mg/ml of proteinase K (2 h, 37 °C); the resulting products were separated on 0.7% agarose gel and detected by ethidium bromide staining.

RNA polymerase activity

IBDV polymerase reactions were performed with dsRNA, VPg–dsRNA complex, RNP, and virions, as described elsewhere[44] but with minor variations. The transcription buffer contained 100 mM Tris–HCl, pH 8.5, 125 mM NaCl, 4 mM $MgCl_2$, 0.01 mM EGTA [ethylene glycol bis(β-aminoethyl ether)*N*,*N*′-tetraacetic acid], 1 mM each of ATP, GTP, and CTP, 0.02 mM UTP, 20 U of RNasin (Promega), and 10 μCi [α-^{32}P]UTP. After incubation of the reaction mixture at 40 °C for 0, 15, 60, or 120 min, the mixture was frozen (−80 °C). Reaction products were thawed at 37 °C, supplemented with 1% SDS, heated at 100 °C for 3 min, incubated (1 min, 4 °C), and digested with 0.2 mg/ml of proteinase K (2 h, 37 °C). Radioactive nucleotides not incorporated into nascent chains were removed using Microspin S-200 HR Sepharose columns (GE Healthcare). Reaction products were resolved by agarose gel electrophoresis and detected with a Storm gel imaging system (Molecular Dynamics). Data were quantitated with Quantity One software (BioRad).

Electron microscopy

Three techniques were used:

(1) Negative staining. Virion particles and partially disrupted virions and RNPs (~5 μl) were applied to glow-discharged carbon-coated grids for 2 min. Samples were negatively stained with 2% (wt/vol) aqueous uranyl acetate. Micrographs were recorded with a JEOL 1200 EXII electron microscope operating at 100 kV at a nominal magnification of ×40,000.

(2) Metal shadowing. Sample adsorption was as described above, except for dsRNA and VPg–dsRNA samples, which were adsorbed in 10 mM and 20 mM magnesium acetate, respectively. They were then air dried and transferred to a Balzers 400-T stage (Bal-Tec AG). Samples were shadowed rotationally with ~60-Å platinum at an angle of 3°, and the replica was reinforced with an ~2-nm carbon layer. Samples were visualized with a JEOL 1010 JEM electron microscope operating at 80 kV, and images were recorded with a Bioscan 792 charge-coupled device camera at a nominal magnification of ×40,000, giving a pixel size of 1.14 nm.

(3) Immunogold labeling. RNP complexes were applied to glow-discharged carbon-coated grids for 2 min to identify VP3 on their outer surface. The grids were then blocked with 5% BSA–PBS for 10 min. Polyclonal rabbit αVP3 antiserum (1/100 in 0.1% BSA–PBS) was incubated for 10 min, followed by three washes with 0.1% BSA–PBS. Protein A conjugated to 5-nm gold particles (1/50; Biocell) was added to the grid for 10 min. Samples were washed twice with PBS and six times with water to eliminate nonspecific binding. The grids were metal shadowed as above.

Acknowledgements

D.L.B. was supported by an FPI fellowship from the Spanish Ministry of Education (MEC). This work was supported by grants BFU 2005-06487 and BFU 2006-09407 from the Spanish Dirección General de Investigación (MEC). We thank C. Mark for editorial help.

Supplementary Data

Supplementary data associated with this article can be found, in the online version, at doi:10.1016/j.jmb.2008.11.029

References

1. Ball, L. A. (2007). Virus replication strategies. In *Fields Virology* (Knipe, D. M., Howley, P. M., Griffin, D. E.,

Lamb, R. A., Martin, M. A., Roizman, B. & Strauss, S. E., eds), 5th edit., vol. 1, pp. 119–139. Lippincott Williams & Wilkins, Philadelphia, PA.
2. Hutvagner, G. & Simard, M. J. (2008). Argonaute proteins: key players in RNA silencing. *Nat. Rev. Mol. Cell Biol.* **9**, 22–32.
3. Lemaire, P. A., Anderson, E., Lary, J. & Cole, J. L. (2008). Mechanism of PKR activation by dsRNA. *J. Mol. Biol.* **381**, 351–360.
4. Reinisch, K. M. (2002). The dsRNA Viridae and their catalytic capsids. *Nat. Struct. Biol.* **9**, 714–716.
5. Chao, J. A., Lee, J. H., Chapados, B. R., Debler, E. W., Schneemann, A. & Williamson, J. R. (2005). Dual modes of RNA-silencing suppression by flock house virus protein B2. *Nat. Struct. Mol. Biol.* **12**, 952–957.
6. Chen, H. Y., Yang, J., Lin, C. & Yuan, Y. A. (2008). Structural basis for RNA-silencing suppression by tomato aspermy virus protein 2b. *EMBO Rep.* **9**, 754–760.
7. Albertini, A. A., Wernimont, A. K., Muziol, T., Ravelli, R. B., Clapier, C. R., Schoehn, G. *et al.* (2006). Crystal structure of the rabies virus nucleoprotein–RNA complex. *Science*, **313**, 360–363.
8. Green, T. J., Zhang, X., Wertz, G. W. & Luo, M. (2006). Structure of the vesicular stomatitis virus nucleoprotein–RNA complex. *Science*, **313**, 357–360.
9. Delmas, B., Kibenge, F. S. B., Leong, J. C., Mundt, E., Vakharia, V. N. & Wu, J. L. (2005). Birnaviridae. In *Virus Taxonomy* (Fauquet, C. M., Mayo, M. A., Maniloff, J., Desselberger, U. & Ball, L. A., eds), pp. 561–569, Elsevier/Academic Press, Amsterdam, The Netherlands.
10. Castón, J. R., Martínez-Torrecuadrada, J. L., Maraver, A., Lombardo, E., Rodríguez, J. F., Casal, J. I. & Carrascosa, J. L. (2001). C terminus of infectious bursal disease virus major capsid protein VP2 is involved in definition of the *T* number for capsid assembly. *J. Virol.* **75**, 10815–10828.
11. Coulibaly, F., Chevalier, C., Gutsche, I., Pous, J., Navaza, J., Bressanelli, S. *et al.* (2005). The birnavirus crystal structure reveals structural relationships among icosahedral viruses. *Cell*, **120**, 761–772.
12. Böttcher, B., Kiselev, N. A., Stel'Mashchuk, V. Y., Perevozchikova, N. A., Borisov, A. V. & Crowther, R. A. (1997). Three-dimensional structure of infectious bursal disease virus determined by electron cryomicroscopy. *J. Virol.* **71**, 325–330.
13. Birghan, C., Mundt, E. & Gorbalenya, A. E. (2000). A non-canonical lon proteinase lacking the ATPase domain employs the Ser–Lys catalytic dyad to exercise broad control over the life cycle of a double-stranded RNA virus. *EMBO J.* **19**, 114–123.
14. Feldman, A. R., Lee, J., Delmas, B. & Paetzel, M. (2006). Crystal structure of a novel viral protease with a serine/lysine catalytic dyad mechanism. *J. Mol. Biol.* **358**, 1378–1389.
15. von Einem, U. I., Gorbalenya, A. E., Schirrmeier, H., Behrens, S. E., Letzel, T. & Mundt, E. (2004). VP1 of infectious bursal disease virus is an RNA-dependent RNA polymerase. *J. Gen. Virol.* **85**, 2221–2229.
16. Pan, J., Vakharia, V. N. & Tao, Y. J. (2007). The structure of a birnavirus polymerase reveals a distinct active site topology. *Proc. Natl Acad. Sci. USA*, **104**, 7385–7390.
17. Maraver, A., Oña, A., Abaitua, F., Gonzalez, D., Clemente, R., Ruiz-Díaz, J. A. *et al.* (2003). The oligomerization domain of VP3, the scaffolding protein of infectious bursal disease virus, plays a critical role in capsid assembly. *J. Virol.* **77**, 6438–6449.
18. Saugar, I., Luque, D., Ona, A., Rodriguez, J. F., Carrascosa, J. L., Trus, B. L. & Caston, J. R. (2005). Structural polymorphism of the major capsid protein of a double-stranded RNA virus: an amphipathic alpha helix as a molecular switch. *Structure*, **13**, 1007–1017.
19. Chevalier, C., Lepault, J., Da Costa, B. & Delmas, B. (2004). The last C-terminal residue of VP3, glutamic acid 257, controls capsid assembly of infectious bursal disease virus. *J. Virol.* **78**, 3296–3303.
20. Garriga, D., Navarro, A., Querol-Audi, J., Abaitua, F., Rodriguez, J. F. & Verdaguer, N. (2007). Activation mechanism of a noncanonical RNA-dependent RNA polymerase. *Proc. Natl Acad. Sci. USA*, **104**, 20540–20545.
21. Maraver, A., Clemente, R., Rodríguez, J. F. & Lombardo, E. (2003). Identification and molecular characterization of the RNA polymerase-binding motif of infectious bursal disease virus inner capsid protein VP3. *J. Virol.* **77**, 2459–2468.
22. Tacken, M. G., Peeters, B. P., Thomas, A. A., Rottier, P. J. & Boot, H. J. (2002). Infectious bursal disease virus capsid protein VP3 interacts both with VP1, the RNA-dependent RNA polymerase, and with viral double-stranded RNA. *J. Virol.* **76**, 11301–11311.
23. Pedersen, T., Skjesol, A. & Jorgensen, J. B. (2007). VP3, a structural protein of infectious pancreatic necrosis virus, interacts with RNA-dependent RNA polymerase VP1 and with double-stranded RNA. *J. Virol.* **81**, 6652–6663.
24. Kochan, G., Gonzalez, D. & Rodriguez, J. F. (2003). Characterization of the RNA-binding activity of VP3, a major structural protein of infectious bursal disease virus. *Arch. Virol.* **148**, 723–744.
25. Casañas, A., Navarro, A., Ferrer-Orta, C., Gonzalez, D., Rodriguez, J. F. & Verdaguer, N. (2008). Structural insights into the multifunctional protein VP3 of birnaviruses. *Structure*, **16**, 29–37.
26. Hjalmarsson, A., Carlemalm, E. & Everitt, E. (1999). Infectious pancreatic necrosis virus: identification of a VP3-containing ribonucleoprotein core structure and evidence for O-linked glycosylation of the capsid protein VP2. *J. Virol.* **73**, 3484–3490.
27. Gorbalenya, A. E., Pringle, F. M., Zeddam, J. L., Luke, B. T., Cameron, C. E., Kalmakoff, J. *et al.* (2002). The palm subdomain-based active site is internally permuted in viral RNA-dependent RNA polymerases of an ancient lineage. *J. Mol. Biol.* **324**, 47–62.
28. Ahlquist, P. (2005). Virus evolution: fitting lifestyles to a *T. Curr. Biol.* **15**, R465–R467.
29. Muller, H. & Nitschke, R. (1987). The two segments of the infectious bursal disease virus genome are circularized by a 90,000-Da protein. *Virology*, **159**, 174–177.
30. Oña, A., Luque, D., Abaitua, F., Maraver, A., Castón, J. R. & Rodríguez, J. F. (2004). The C-terminal domain of the pVP2 precursor is essential for the interaction between VP2 and VP3, the capsid polypeptides of infectious bursal disease virus. *Virology*, **322**, 135–142.
31. Chevalier, C., Lepault, J., Erk, I., Da Costa, B. & Delmas, B. (2002). The maturation process of pVP2 requires assembly of infectious bursal disease virus capsids. *J. Virol.* **76**, 2384–2392.
32. Jeffery, C. J. (2004). Molecular mechanisms for multitasking: recent crystal structures of moonlighting proteins. *Curr. Opin. Struct. Biol.* **14**, 663–668.
33. Tompa, P., Szasz, C. & Buday, L. (2005). Structural disorder throws new light on moonlighting. *Trends Biochem. Sci.* **30**, 484–489.
34. Nardini, M., Svergun, D., Konarev, P. V., Spano, S., Fasano, M., Bracco, C. *et al.* (2006). The C-terminal

domain of the transcriptional corepressor CtBP is intrinsically unstructured. *Protein Sci.* **15**, 1042–1050.
35. Gonzalez, D., Rodriguez, J. F. & Abaitua, F. (2005). Intracellular interference of infectious bursal disease virus. *J. Virol.* **79**, 14437–14441.
36. Vayda, M. E., Rogers, A. E. & Flint, S. J. (1983). The structure of nucleoprotein cores released from adenovirions. *Nucleic Acids Res.* **11**, 441–460.
37. Egelman, E. H., Wu, S. S., Amrein, M., Portner, A. & Murti, G. (1989). The Sendai virus nucleocapsid exists in at least four different helical states. *J. Virol.* **63**, 2233–2243.
38. Schoehn, G., Mavrakis, M., Albertini, A., Wade, R., Hoenger, A. & Ruigrok, R. W. (2004). The 12 Å structure of trypsin-treated measles virus N-RNA. *J. Mol. Biol.* **339**, 301–312.
39. Maclellan, K., Loney, C., Yeo, R. P. & Bhella, D. (2007). The 24-angstrom structure of respiratory syncytial virus nucleocapsid protein–RNA decameric rings. *J. Virol.* **81**, 9519–9524.
40. Klumpp, K., Ruigrok, R. W. & Baudin, F. (1997). Roles of the influenza virus polymerase and nucleoprotein in forming a functional RNP structure. *EMBO J.* **16**, 1248–1257.
41. Patton, J. T., Silvestri, L. S., Tortorici, M. A., Vasquez-Del Carpio, R. & Taraporewala, Z. F. (2006). Rotavirus genome replication and morphogenesis: role of the viroplasm. *Curr. Top. Microbiol. Immunol.* **309**, 169–187.
42. Schwartz, M., Chen, J., Janda, M., Sullivan, M., den Boon, J. & Ahlquist, P. (2002). A positive-strand RNA virus replication complex parallels form and function of retrovirus capsids. *Mol. Cell*, **9**, 505–514.
43. Song, J. J., Smith, S. K., Hannon, G. J. & Joshua-Tor, L. (2004). Crystal structure of Argonaute and its implications for RISC slicer activity. *Science*, **305**, 1434–1437.
44. Spies, U., Muller, H. & Becht, H. (1987). Properties of RNA polymerase activity associated with infectious bursal disease virus and characterization of its reaction products. *Virus Res.* **8**, 127–140.